

## Original Article

## Effect of Soothing Gan (Liver) and Invigorating Pi (Spleen) Recipes on TLR4-p38 MAPK Pathway in Kupffer Cells of Non-alcoholic Steatohepatitis Rats\*

GONG Xiang-wen, XU Yong-jian, YANG Qin-he, LIANG Yin-ji,  
ZHANG Yu-pei, WANG Guan-long, and LI Yuan-yuan

**ABSTRACT** **Objective:** To investigate the mechanism of inflammatory-mediated toll-like receptor 4 (TLR4)-p38 mitogen-activated protein kinase (p38 MAPK) pathway in Kupffer cells (KCs) of non-alcoholic steatohepatitis (NASH) rats and the intervention effect of soothing Gan (Liver) and invigorating Pi (Spleen) recipes on this pathway. **Methods:** After 1 week of acclimatization, 120 Sprague-Dawley male rats were randomly divided into 8 groups using a random number table ( $n=15$  per group): normal group, model group, low-dose Chaihu Shugan Powder (柴胡疏肝散, CHSG) group (3.2 g/kg), high-dose CHSG group (9.6 g/kg), low-dose Shenling Baizhu Powder (参苓白术散, SLBZ) group (10 g/kg), high-dose SLBZ (30 g/kg) group, and low- and high-dose integrated recipe (L-IR, H-IR) groups. All rats in the model and treatment groups were fed with a high-fat diet (HFD). The treatments were administrated by gastrogavage once daily and lasted for 26 weeks. The liver tissues were detected with hematoxylin-eosin (HE) and oil red O staining. Levels of liver lipids, serum lipids and transaminases were measured. KCs were isolated from the livers of rats to evaluate the mRNA expressions of TLR4 and p38 MAPK by real-time fluorescence quantitative polymerase chain reaction, and proteins expressions of TLR4, p-p38 MAPK and p38 MAPK by Western blot. Levels of inflammatory cytokines including tumor necrosis factor  $\alpha$  (TNF- $\alpha$ ), interleukin (IL)-1 and IL-6 in KCs were measured by enzyme-linked immunosorbent assay. **Results:** After 26 weeks of HFD feeding, HE and oil red O staining showed that the NASH model rats successfully reproduced typical pathogenesis and histopathological features. Compared with the normal group, the model group exhibited significant increases in body weight, liver weight, liver index, serum levels of total cholesterol (TC), triglyceride (TG), low-density lipoprotein cholesterol, and aspartate aminotransferase as well as TC and TG levels in liver tissues, and significant decrease in serum level of high-density lipoprotein cholesterol ( $P<0.05$  or  $P<0.01$ ), while those indices were significantly ameliorated in the H-IR group ( $P<0.05$  or  $P<0.01$ ). Higher levels of TNF- $\alpha$ , IL-1 and IL-6 in KCs were observed in the model group compared with the normal group ( $P<0.01$ ). Significant decreases in TNF- $\alpha$ , IL-1 and IL-6 were observed in the H-SLBZ, H-IR and L-IR groups compared with the model group ( $P<0.05$  or  $P<0.01$ ). The mRNA expressions of TLR4 and p38 MAPK and protein expressions of TLR4, p38 MAPK and p-p38 MAPK in KCs in the model group were significantly higher than the normal group ( $P<0.01$ ), while those expression levels in the L-IR and H-IR groups were significantly lower than the model group ( $P<0.05$  or  $P<0.01$ ). **Conclusions:** Inflammation in KCs might play an important role in the pathogenesis of NASH in rats. The data demonstrated the importance of TLR4-p38MAPK signaling pathway in KCs for the anti-inflammatory effect of soothing Gan and invigorating Pi recipes.

**KEYWORDS** non-alcoholic steatohepatitis, soothing Gan (Liver) and invigorating Pi (Spleen) recipes, Kupffer cell, toll-like receptor 4-p38 mitogen-activated protein kinase signaling pathway, inflammation, Chinese medicine

Non-alcoholic fatty liver disease (NAFLD) is one of the most prevalent liver diseases in the developed countries and occurs in 20%–25% of the general population.<sup>(1,2)</sup> The pathological changes in the NAFLD range from simple non-progressive steatosis to non-alcoholic steatohepatitis (NASH). These conditions can progress to cirrhosis, hepatocellular carcinoma,

©The Chinese Journal of Integrated Traditional and Western Medicine Press and Springer-Verlag Berlin Heidelberg 2018  
 \*Supported by the National Natural Science Foundation of China (No. 30973694)

School of Chinese Medicine, Jinan University, Guangzhou (510632), China

Correspondence to: Prof. YANG Qin-he, Tel: 86-20-85226197, E-mail: [tyangqh@jnu.edu.cn](mailto:tyangqh@jnu.edu.cn)

DOI: <https://doi.org/10.1007/s11655-018-2829-6>

and liver failure with increased hepatic-related mortality.<sup>(3)</sup> NASH may play a key role in disease progression and the development of complications in NAFLD.<sup>(4)</sup> Therefore, studies investigating the prevention and treatment of NASH are very important.

Clinically, high fat and sugar intakes (Western-style diet) are thought to be of particular relevance in metabolic syndrome, hepatic steatosis and NASH. For that reason, a high-fat diet (HFD) is commonly used in the experimental induction of NAFLD.<sup>(5,6)</sup> A previous study has shown that 16 weeks of HFD feeding could induce NASH in rats.<sup>(7)</sup> The various stages of NAFLD may reveal inflammation changes. Hence, we used NASH rats that induced by 26-week HFD feeding to explore the pathological evolution in the different periods of NASH.

Since the pathogenesis of NAFLD is not fully elucidated, there is a lack of a consensus regarding the most effective and appropriate pharmacologic therapy.<sup>(8)</sup> Data from the World Health Organization (WHO) has shown that approximately 80% of the population in some African and Asian countries and 38% in the America depend primarily on complementary and alternative medicine for the prevention, protection and treatment of diseases.<sup>(4)</sup> Chinese medicine (CM) is an important component of complementary and alternative medicine. Evidence-based medicine has demonstrated that application of herbal treatment for NAFLD has received increasing attention due to its wide availability, minimal side effects, and proven therapeutic mechanisms and benefits.<sup>(9)</sup> Based on the CM theory, Gan (Liver) qi stagnation and Pi (Spleen) deficiency is the basic syndrome of NAFLD. Accordingly, soothing Gan and invigorating Pi have become the basic treatment methods in NAFLD.<sup>(10)</sup> Chaihu Shugan Powder (柴胡疏肝散, CHSG) and Shenling Baizhu Powder (参苓白术散, SLBZ) are ancient classical formulae to soothe Gan and invigorate Pi, respectively.

Toll-like receptor 4 (TLR4)-p38 mitogen-activated protein kinase (MAPK) is an important pro-inflammatory transcription factor that plays a critical role in the regulation of various important genes in cellular responses.<sup>(11)</sup> Our previous study has shown that the over-expressions of TLR4, p38 MAPK and p-p38 MAPK in Kupffer cells (KCs) isolated from NASH rats induced by 16-week HFD, which

preliminarily revealed the relationship between NAFLD and TLR4-p38 MAPK pathway.<sup>(12)</sup> Therefore, in this research, we focused on the evolution of NASH in rats undergoing HFD feeding for 26 weeks, and studied the effects of soothing Gan and invigorating Pi recipes on inflammatory markers and proteins involved in TLR4-p38 MAPK pathway in KCs of NASH rats to explore part of the underlying mechanisms.

## METHODS

### Animals

A total of 120 Sprague-Dawley rats (male, 6 weeks old, 200 ± 20 g, specific pathogen-free grade) were obtained from the Laboratory Animal Research Center of Guangzhou University of Traditional Chinese Medicine [license No. SCXK(Yue)2008-0020]. The use of animals in this study was approved by Laboratory Animal Ethics Committee of Jinan University (No. 20140305006). The rats were housed separately at Jinan University Animal Administration Laboratory, 5 per cage in an environmentally controlled facility (22–26 °C and 50%–70% humidity) with a 12-h light/dark cycle and free access to rat chow and water.

### Drugs

CHSG was composed of 7 Chinese herbs: *Radix Bupleuri* 6 g, *Pericarpium Citri Reticulatae* 6 g, *Rhizoma Chuanxiong* 5 g, *Rhizoma Cyperi* 5 g, *Fructus Aurantii* 5 g, *Paeonia lactiflora* Pall 5 g, and *Radix Glycyrrhizae* 3 g (0.32 g crude drug/mL decoction). SLBZ was composed of 10 Chinese herbs: *Radix Ginseng* 15 g, *Radix Platycodi* 6 g, *Rhizoma Atractylodes Alba* 15 g, *Poria* 15 g, *Semen Coicis* 9 g, *Fructus Amomi* 6 g, *Rhizoma Dioscorese* 15 g, *Semen Dolichoris Albae* 12 g, *Semen Nelumbinis* 9 g, and *Radix Glycyrrhizae* 9 g (1 g crude drug/mL decoction). Integrated recipes (IRs) contained a mixture of CHSG and SLBZ at a ratio of 1:1. All CMs were formula granules provided by China Resources Sanjiu Medical and Pharmaceutical Co., Ltd. (batch No. 1005001S). The formula granules were dissolved in distilled water and refrigerated at –4 °C.

### Grouping and Treatment

After 1 week of acclimatization, rats were randomly divided into 8 groups using a random number table ( $n=15$  per group): (1) normal group: fed with standard rat chow and water; (2) model group: fed with HFD (composed of regular chow 88 %, axungia porci 10%, cholesterol 1.5%, and bile salt 0.5%) and water;<sup>(13)</sup> (3) low-dose CHSG group (L-CHSG, 3.2 g/kg); (4) high-dose

CHSG group (H-CHSG, 9.6 g/kg); (5) low-dose SLBZ group (L-SLBZ, 10 g/kg); (6) high-dose SLBZ group (H-SLBZ, 30 g/kg); (7) and (8) low- and high-dose IR groups (L-IR, H-IR).<sup>(14)</sup> All rats in the treatment groups were fed with HFD and administrated with decoction (1 mL/100 g body weight by gastrogavage) once daily. Low dose equaled a human clinical equivalent dosage, and high dose was a 3-fold volume of the low dose. The treatment lasted for 26 weeks.

### Reagents

Enzyme-linked immunosorbent assay (ELISA) kits for tumor necrosis factor  $\alpha$  (TNF- $\alpha$ , No. 24122012-002), interleukin (IL)-1 (No. ZGAHBZAB01) and IL-6 (No. ZIBIBZAB02) were purchased from ExCell Biology (Shanghai, China). TRIZOL reagent (No. R0016) was purchased from Beyotime Biotechnology (Shanghai, China). TLR4 antibody (No. 0002), p-p38 MAPK antibody (No.0010) and p38 MAPK antibody (No.0004) were purchased from Cell Signaling Technology (Danvers, USA). Lysozyme antibody (No. Y-Bo-07J26C) was purchased from Boster Biological Technology (Wuhan, China).

### Body Weight, Liver Weight and Liver Index

Body weight was measured at the end of the study. Rats were anesthetized by intraperitoneal injection of 3% pentobarbital (0.2 mL/100 g body weight), then the livers of rats were immediately removed and weighed. The liver index was calculated as liver weight/body weight.

### Histopathological Examination of Liver

The paraffin-embedded liver tissues (approximately 1 cm  $\times$  1 cm  $\times$  0.5 cm) were selected from the same part of liver, approximately 0.5 cm from the edge of the right hepatic lobule, and then examined by hematoxylin-eosin (HE) staining. The steatosis, fibrosis and inflammation of NASH were observed by light microscopy (DM6000, Leica, Germany). Frozen sections were prepared and oil red O staining was used to observe the distribution of lipid droplets in liver cells.

### Biochemical Test in Serum and Liver Tissues

After rats were anesthetized, blood samples were collected from abdominal aorta and then centrifuged at 3,000 r/min for 10 min at 4 °C. The clear supernatants were collected to measure total cholesterol (TC), triglyceride (TG), high-density lipoprotein cholesterol

(HDL-C), low-density lipoprotein cholesterol (LDL-C), aspartate aminotransferase (AST) and alanine aminotransferase (ALT) in serum by an automatic biochemical analyzer (AU400, Olympus, Japan). Liver tissues were placed in isopropanol, liver homogenates were manufactured using a homogenizer (Tissue-Lyser II, QIAGEN, Germany), and then clear supernatants were collected. Levels of TC and TG in the liver tissues were also determined.

### Isolation and Identification of KCs

KCs were isolated and identified from 6 rats in each group as previously described.<sup>(15)</sup> The viability of KCs was tested by trypan blue, and the purity was assessed by flow cytometry method using lysozyme antibody.

### Determination of Inflammatory Cytokines in KCs

KCs ( $1 \times 10^6$  /mL) were centrifuged and washed with phosphate-buffered saline (PBS) 3 times, and then lysed using a sonicator at 10,000 r/min, 4 °C for 15 min. Clear supernatants were collected to determine the levels of TNF- $\alpha$ , IL-1 and IL-6.

### Determination of TLR4 and p38 MAPK mRNA Expressions in KCs Using Real-Time Quantitative Polymerase Chain Reaction Method

Total RNA was extracted from KCs using TRIZOL reagent according to manufacturer's instruction. The integrity of each RNA sample was evaluated by agarose gel electrophoresis, and its purity and concentration were assayed. Then total RNA was reversely transcribed to cDNA. The primers of TLR4 and p38 MAPK and glyceraldehyde-3-phosphate dehydrogenase (GAPDH) were designed and synthesized by Shanghai Generay Biological Engineering Co., Ltd. (China). GAPDH was used as the internal control. The sequences of the primers were as follows: TLR4: 5'-CGCTCTGGCATCATCTTCATTG-3' (forward) and 5'-TGCCTCCCCAGAGCATTGTC-3' (reverse), 148 bp; p38 MAPK: 5'-ACCACGACCCTGATGATGAGC-3' (forward) and 5'-GGTCAGGCTCTTCCATTTCGTCT-3' (reverse), 193 bp; GAPDH: 5'-GATCCCGCTAACATCAAATG-3' (forward) and 5'-GAGGGAGTTGTCATATTTCTC-3' (reverse), 134 bp. The reaction conditions were as follows: (1) pre-denaturation for 10 s at 95 °C; (2) denaturation for 5 s at 95 °C; (3) GAPDH 55 °C, TLR4 58 °C, p38 MAPK 60 °C, renaturation for 20 s; (4) extension for 40 s at 60 °C, (2)–(4) repeated 39 times; (5)

analysis of solubility curve, 72–95 °C for 5–10 s. After the reaction was finished, the results were analyzed using Opticon Monitor 3.1 software (Bio-Rad Laboratories, Inc., USA), and the formula  $2^{-\Delta\Delta Ct}$  was used for relative quantification.

### Determination of TLR4, p-p38 MAPK and p38 MAPK Protein Expressions in KCs Using Western Blot Analysis

The proteins of TLR4, p-p38 MAPK, p38 MAPK and GAPDH in KCs were measured by Western blot analysis. GAPDH was used as an internal control. KCs were split in radioimmunoprecipitation assay (RIPA) lysis buffer and centrifuged at 12,000 r/min for 5 min at 4 °C and the supernatants were collected. The concentration of supernatant protein was determined by bicinchoninic acid (BCA) protein assay. Protein preparations were subjected to 10% sodium dodecylsulfate polyacrylamide gel electrophoresis (SDS-PAGE) and transferred to polyvinylidene difluoride (PVDF) membrane. After transfer, membrane was blocked in 5% skim milk in Tris-buffered saline tween-20 (TBST) and incubated overnight at 4 °C with specific primary antibodies. Then horseradish peroxidase (HRP) conjugated goat-anti-rabbit antibody was added and incubated at room temperature for 1 h. After being washed 3 times in TBST, the PVDF membrane was put into a developer and exposed to X-ray film. The films were scanned and analyzed by a gel image processing system.

### Statistical Analysis

Data were expressed as mean  $\pm$  standard deviation ( $\bar{x} \pm s$ ). Data were analyzed using Statistical Package for the Social Sciences v13.0 Software (SPSS, USA). One-way analysis of variance and Tukey's test were used to determine the statistical significance of the differences.  $P < 0.05$  was considered statistically significant.

## RESULTS

### Body Weight, Liver Weight and Liver Index

After 26 weeks of HFD feeding, the model group

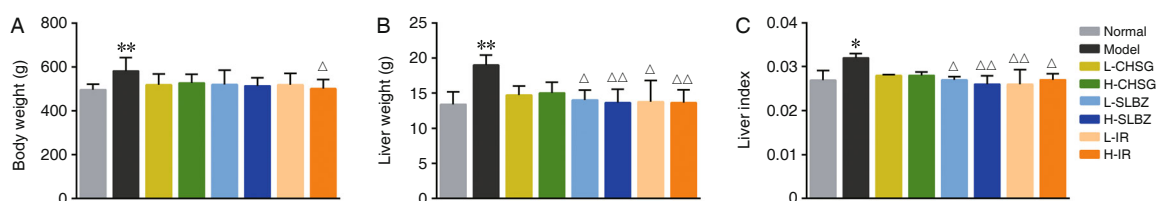


Figure 1. Body Weight, Liver Weight and Liver Index in All Groups

Notes: \* $P < 0.05$ , \*\* $P < 0.01$  vs. normal group;  $\Delta P < 0.05$ ,  $\Delta\Delta P < 0.01$  vs. model group

exhibited significant increases in body weight, liver weight and liver index compared with the normal group ( $P < 0.05$  or  $P < 0.01$ ). Compared with the model group, H-IR significantly decreased the body weight ( $P < 0.05$ ), while SLBZ and IR significantly decreased the liver weight and liver index ( $P < 0.05$  or  $P < 0.01$ , Figure 1).

### Observation on Morphology of Liver Tissues of Rats

In the normal group, hepatocyte nuclei were blue, and cytoplasm was red-stained with no lipid vacuoles. The hepatic lobules and hepatic cords had clear structures and regular arrangement. There was no spotty necrosis or inflammatory infiltration. In the model group, the central vein and portal area had diffused lipid vacuoles. Hepatocytes were obviously swelling or even ballooning with many lipid vacuoles in the cytoplasm. The irregular hepatic lobules and hepatic cords were observed. Inflammatory infiltrates were found in the hepatic lobules and portal areas. Compared with the model group, the structure arrangement, morphological features, macrovesicular lipid droplets, ballooning, inflammatory infiltrates, and spotty necrosis were improved by various degrees in all treatment groups. H-IR had the most significant effect on liver histopathology (Figure 2).

Frozen sections were stained with Oil red O. In the normal group, hepatocyte nuclei were blue and had no lipid droplets in the cytoplasm. In the model group, there were diffused red lipid droplets in hepatocytes. The nuclei were squeezed to one side by lipid droplets. In the H-CHSG, L-CHSG, H-SLBZ, and L-SLBZ groups, large clumps of red lipid droplets were observed. The red lipid droplets in the H-IR and L-IR groups were significantly fewer than those in the model group and other treatment groups, especially the H-IR group (Figure 3).

### Levels of TC, TG, HDL-C and LDL-C in Serum

Compared with the normal group, the levels of TC, TG and LDL-C were significantly increased while

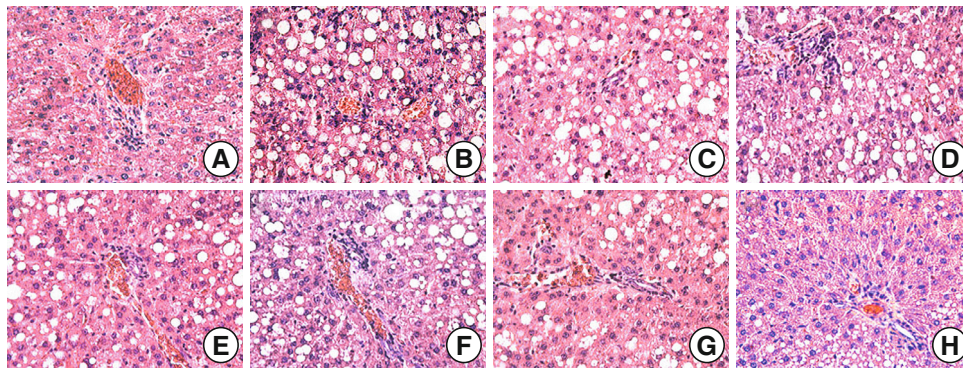


**Figure 2. Histological Changes of Liver Sections in All Groups (HE staining, ×200)**

Notes: A: normal group; B: model group; C: L-CHSG group; D: H-CHSG group; E: L-SLBZ group; F: H-SLBZ group; G: L-IR group; H: H-IR group

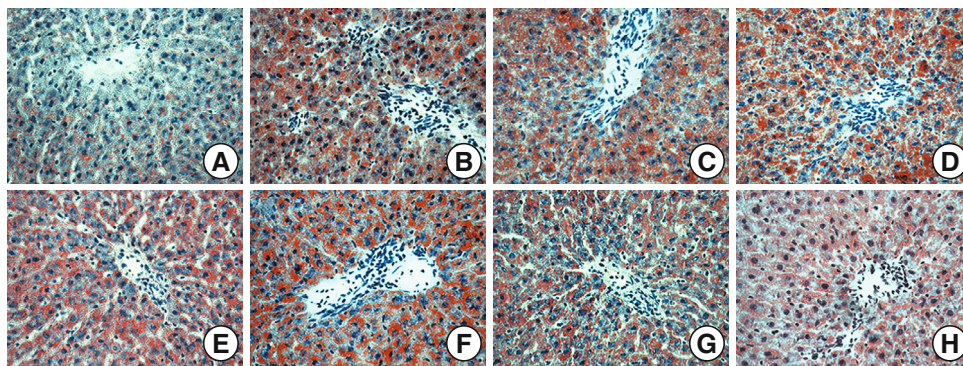


**Figure 3. Histological Changes of Liver Sections in All Groups (Oil red O staining, ×100)**

Notes: A: normal group; B: model group; C: L-CHSG group; D: H-CHSG group; E: L-SLBZ group; F: H-SLBZ group; G: L-IR group; H: H-IR group

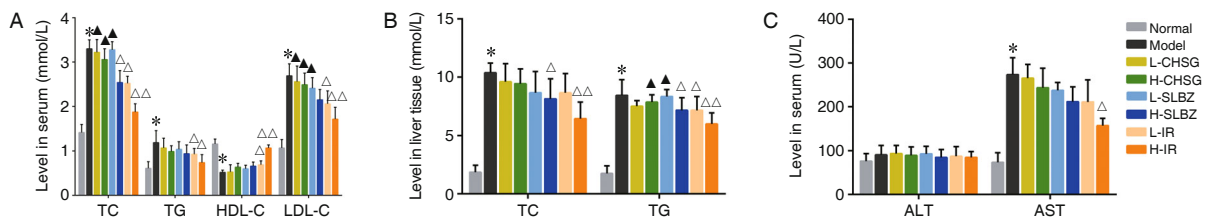


**Figure 4. Levels of Liver Lipids, Serum Lipids and Transaminases in All Groups**

Notes: \* $P < 0.01$  vs. normal group;  $\Delta P < 0.05$ ,  $\Delta\Delta P < 0.01$  vs. model group;  $\Delta P < 0.05$  vs. H-IR group

the HDL-C level was significantly decreased in the model group ( $P < 0.01$ ). The TC levels of H-SLBZ, L-IR and H-IR groups were significantly lower than those of the model group ( $P < 0.05$  or  $P < 0.01$ ). The TG and LDL-C levels of L-IR and H-IR groups were significantly lower than those of the model group ( $P < 0.05$  or  $P < 0.01$ ), while the HDL-C levels of L-IR and H-IR groups were significantly higher than those of the model group ( $P < 0.05$  or  $P < 0.01$ , Figure 4A).

#### Levels of TC and TG in Liver Tissues

Compared with the normal group, the TC and TG levels in liver tissues were significantly higher in the model group ( $P < 0.01$ ). Compared with the model

group, the TC levels in liver tissues in H-SLBZ and H-IR groups were significantly decreased ( $P < 0.05$  or  $P < 0.01$ ). The TG levels in liver tissues in H-SLBZ, L-IR and H-IR groups were significantly lower than those in the model group ( $P < 0.05$  or  $P < 0.01$ , Figure 4B).

#### Levels of ALT and AST in Serum

Compared with the normal group, the serum AST levels were increased in the model group ( $P < 0.01$ ). Compared with the model group, AST levels of H-IR group was significantly decreased ( $P < 0.05$ , Figure 4C).

#### Purity and Viability of KCs

The viability of KCs was  $>95\%$  as tested by

trypan blue. The purity of KCs was 91.21% (Figures 5A and 5B).

### Changes in Inflammatory Cytokines in KCs

Higher levels of TNF- $\alpha$ , IL-1 and IL-6 in KCs were observed in the model group than the normal group ( $P<0.01$ ). Compared with the model group, significant decreases in TNF- $\alpha$ , IL-1 and IL-6 were observed in the H-SLBZ, H-IR and L-IR groups ( $P<0.05$  or  $P<0.01$ ), and TNF- $\alpha$  level in the L-SLBZ group and IL-1 level in the H-CHSG group were also decreased ( $P<0.05$ , Figure 5C).

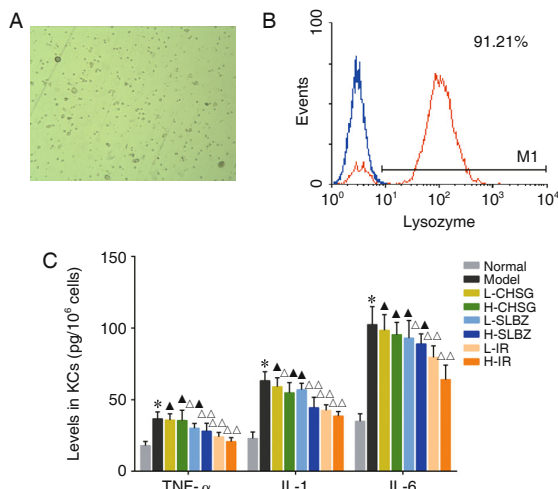


**Figure 5. Levels of TNF- $\alpha$ , IL-1 and IL-6 in Isolated KCs**

Notes: A: Isolated rat KCs were cultured for 3 h ( $\times 100$ ); B: the purity of KCs was 91.21%; C: levels of TNF- $\alpha$ , IL-1 and IL-6 in KCs. \* $P<0.01$  vs. normal group;  $\Delta P<0.05$ ,  $\Delta\Delta P<0.01$  vs. model group;  $\Delta P<0.05$  vs. H-IR group

### TLR4 and p38 MAPK mRNA Expressions in the KCs of Rats

Compared with the normal group, the mRNA levels of TLR4 and p38 MAPK in the model group increased 8.33 and 10.58 folds, respectively ( $P<0.01$ ). The mRNA levels of TLR4 and p38 MAPK in L-IR and H-IR groups were significantly lower than the model group ( $P<0.05$  or  $P<0.01$ , Table 1).

### TLR4, p38 MAPK and p-p38 MAPK Protein Expressions in the KCs of Rats

The expressions of TLR4, p38 MAPK and p-p38 MAPK protein in KCs of the model group were significantly increased compared with the normal group ( $P<0.01$ ). The expressions of TLR4, p38 MAPK and p-p38 MAPK in H-SLBZ, L-IR and H-IR groups were significantly lower than the model group ( $P<0.05$  or  $P<0.01$ , Figure 6).

**Table 1. Expressions of TLR4 and p38 MAPK mRNA in KCs [Median (min-max),  $n=6$ ]**

Group	TLR4	p38 MAPK
Normal	1 (0.42–2.37)	1 (0.32–3.12)
Model	8.33 (3.71–18.76)*	10.58 (1.96–62.68)*
L-CHSG	7.14 (3.09–16.56)	9.53 (2.28–39.67)
H-CHSG	6.34 (3.03–13.18)	9.08 (3.23–25.46)
L-SLBZ	6.51 (3.05–13.83)	9.13 (3.63–22.94)
H-SLBZ	6.18 (3.14–12.21)	7.09 (1.64–30.91) $\Delta\Delta$
L-IR	6.09 (2.65–8.33) $\Delta$	6.72 (1.51–29.65) $\Delta$
H-IR	5.32 (1.98–14.22) $\Delta$	5.06 (1.42–17.75) $\Delta\Delta$

Notes: The data are presented as relative to control. \* $P<0.01$  vs. normal group;  $\Delta P<0.05$ ,  $\Delta\Delta P<0.01$  vs. model group;  $\Delta P<0.05$  vs. H-IR group

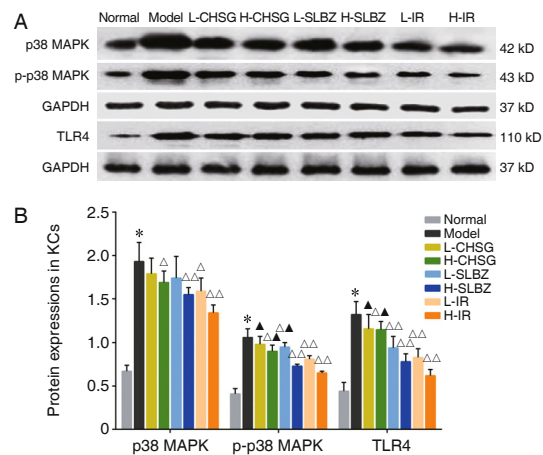


**Figure 6. Expressions of p38 MAPK, p-p38 MAPK and TLR4 Protein in KCs ( $\bar{x} \pm s$ ,  $n=6$ )**

Notes: A: Western blot analysis of p38 MAPK, p-p38 MAPK and TLR4 protein in KCs. B: Graphic presentation of relative expressions of p38 MAPK, p-p38 MAPK and TLR4 protein. \* $P<0.01$  vs. normal group;  $\Delta P<0.05$ ,  $\Delta\Delta P<0.01$  vs. model group;  $\Delta P<0.05$  vs. H-IR group

## DISCUSSION

NASH is a leading condition that results in hepatocirrhosis and liver cancer.<sup>(16,17)</sup> Although the pathogenesis of NASH remains unclear, it is considered to be associated with lipid metabolic disorders, insulin resistance, oxidative stress and secretion of inflammatory cytokines. With the development of NASH, lipid metabolic disorders and secretion of inflammatory cytokines occur, which lead to liver inflammation, fibrosis and even hepatocirrhosis.<sup>(18)</sup> In this study, HE and oil red O staining demonstrated that HFD feeding induced rat model of NASH successfully and replicated several typical histopathological characteristics of NASH in humans. Additionally, the levels of liver lipids, serum lipids and liver function were obviously increased.

However, fibrosis and even hepatocirrhosis were not been observed during the 26 weeks. Consequently, these results suggest that the NASH model induced by 26-week HFD was more severe than the 16-week NASH model, but severe fibrosis and hepatocirrhosis were not observed.

KCs are hepatic macrophages that account for 80%–90% of total fixed tissue macrophages in the body.<sup>(19)</sup> According to the "gut-liver axis" hypothesis, KCs play an important role in liver physiological homeostasis and innate immune system.<sup>(20,21)</sup> KCs are associated with the proinflammatory response and produce associated cytokines, such as IL-6, IL-8, IL-23, and TNF- $\alpha$ . Cytokines act as protective mediators for the recovery of normal liver functions. However, excessive activation of KCs may also result in exacerbation of the damage.<sup>(22,23)</sup> Studies have shown that the inflammation in KCs plays a key role in NASH.<sup>(24)</sup> In this study, the TNF- $\alpha$ , IL-1 and IL-6 levels of KCs increased dramatically in NASH model rats. These findings suggest that increases of TNF- $\alpha$ , IL-1 and IL-6 in KCs were closely related to the degree of inflammatory injury.

Previous studies indicated that the expression of inflammatory factors was closely related to TLR4-p38 MAPK pathway.<sup>(12,25)</sup> After stimulation from conditions such as lipid metabolic disorders, intestinal endotoxemia and other factors, TLR4 is the main receptor in the lipopolysaccharide (LPS)-mediated immune response.<sup>(26)</sup> After TLR4 is integrated with LPS, p38 MAPK protein is phosphorylated, leading to the release of inflammatory factors and starting cell damage mechanism.<sup>(27,28)</sup> Moreover, the activated TLR4 pathway plays a critical role in the inflammatory immune response of NASH.<sup>(29)</sup> In this study, overexpression of mRNAs and proteins related to TLR4-p38 MAPK pathway was observed, suggesting that the activation of TLR4-p38 MAPK-pathway in KCs was induced by HFD. The increased levels of TNF- $\alpha$ , IL-6 and IL-8 in KCs might be caused by the activation of this pathway in KCs. This finding was consistent with our previous research.<sup>(12)</sup> Therefore, we can speculate that TLR4-p38 MAPK pathway also induces inflammation in the progression of NASH.

Currently, medicinal herbs such as CM have received increasing attention as an alternative source of treatment for various diseases.<sup>(30)</sup> We

previously demonstrated that stagnation of Gan qi and Pi deficiency comprise the basic pathogenesis of NAFLD, and soothing Gan and invigorating Pi recipes should be used throughout the disease course.<sup>(10,31)</sup> According to epidemiological research, the syndrome of stagnation of Gan qi and Pi deficiency is one of the most common syndromes of NAFLD in China (the proportion is 34.7%).<sup>(32)</sup> Therefore, the syndrome of stagnation of Gan qi and Pi deficiency has been considered as an important syndrome according to expert consensus regarding NAFLD.<sup>(33)</sup>

CHSG and SLBZ were classical formulae of CM and have been used to treat diseases for a thousand years. According to CM chemistry, the ten effective components in CHSG and SLBZ by high performance liquid chromatography include saikosaponin A, paeoniflorin, hesperidin, ferulic acid, paeoniflorin, liquorice glycosides, naringin, hesperidin, new hesperidin and ginsenosides,<sup>(34-37)</sup> which may be the effective components for treating NAFLD.

Our previous studies showed that soothing Gan and invigorating Pi recipes are effective in preventing and treating NASH.<sup>(12,25)</sup> This efficacy has been demonstrated by various methods including meta-analysis, data mining, clinical studies and experimental researches.<sup>(38-42)</sup> In this study, the effect of H-IR were better than the other treatments. Therefore, we speculate that the pathogenesis of NASH might be closely related to the syndrome of stagnation of Gan qi and Pi deficiency. Consistent with a previous study,<sup>(12)</sup> this result showed that syndrome of NASH due to Pi deficiency could transform into stagnation of Gan qi and Pi deficiency. Additionally, these findings indicated that IR had a significant effect on anti-NASH. However, whether higher dose of IR could be applied in clinical treatment should be further investigated.

This study revealed that the activation of TLR4-p38 MAPK pathway in KCs might be related to the release of inflammatory cytokines such as TNF- $\alpha$ , IL-1 and IL-6 in NASH rats induced by HFD for 26 weeks. High-dose IR might exert a significant anti-inflammatory effect on KCs of HFD-induced NASH rats by suppressing the TLR4-p38 MAPK pathway. The TLR4-p38MAPK pathway might be an effective target for IR. This result was consistent with the 16-week NASH model. However, the pathogenesis

of NASH might be closely related to the syndrome of stagnation of Gan qi and Pi deficiency developed in the 26-week model, reflecting the CM theory of "Treating the same disease with different methods".

### Conflict of Interest

The authors claimed no potential conflicts of interest relevant to this article.

### Author Contributions

Yang QH and Xu YJ conceived and designed the study. Xu YJ, Wang GL and Li YY carried out the experiment. Liang YJ and Zhang YP analyzed the data. Gong XW and Xu YJ wrote the paper. All authors read and approved the final manuscript.

## REFERENCES

- Ritze Y, Böhle M, Haub S, Hubert A, Enck P, Zipfel S, et al. Role of serotonin in fatty acid-induced non-alcoholic fatty liver disease in mice. *BMC Gastroenterol* 2013;13:169.
- Vernon G, Baranova A, Younossi ZM. Systematic review: the epidemiology and natural history of non-alcoholic fatty liver disease and non-alcoholic steatohepatitis in adults. *Aliment Pharmacol Ther* 2011;34:274-285.
- Korish AA, Arafah MM. Camel milk ameliorates steatohepatitis, insulin resistance and lipid peroxidation in experimental non-alcoholic fatty liver disease. *BMC Complement Altern Med* 2013;13:264.
- Wree A, Broderick L, Canbay A, Hoffman HM, Feldstein AE. From NAFLD to NASH to cirrhosis—new insights into disease mechanisms. *Nat Rev Gastroenterol Hepatol* 2013;10:627-636.
- De Wit NJ, Afman LA, Mensink M. Phenotyping the effect of diet on non-alcoholic fatty liver disease. *J Hepatol* 2012;57:1370-1373.
- Mukundh NB, Muralidharan P, Balamurugan G. Antihyperlipidemic activity of *Pedaliium murex* (Linn) fruits on high fat diet fed rats. *Int J Pharmacol* 2008;4:310-313.
- Yang QH, Xu YJ, Feng GF, Hu CF, Zhang YP, Cheng SB, et al. p38 MAPK signal pathway involved in anti-inflammatory effect of Chaihu-shugan-san and Shen-ling-bai-zhu-san on hepatocyte in non-alcoholic steatohepatitis rats. *Afr J Tradit Complement Altern Med* 2013;11:213-221.
- Tomeno W, Yoneda M, Imajo K, Ogawa Y, Kessoku T, Saito S, et al. Emerging drugs for non-alcoholic steatohepatitis. *Expert Opin Emerg Drugs* 2013;18:279-290.
- Li ZZ, Xue J, Chen P, Chen L, Yan S, Liu L. Prevalence of nonalcoholic fatty liver disease in mainland of China: a meta-analysis of published studies. *J Gastroenterol Hepatol* 2014;29:42-51.
- Yang QH, Lin JS, Ping HH, Wen CY. Thinking and countermeasures of prevention and treatment of nonalcoholic fatty liver disease in traditional Chinese medicine. *J Tradit Chin Med (Chin)* 2007;48:746-748.
- Li YQ, Yang QH, Xie WN, Ji GY. Clinical study on soothing Liver and invigorating Spleen method in treating of non-alcoholic fatty liver disease in 35 cases. *J Tradit Chin Med (Chin)* 2007;48:824-825.
- Yang QH, Xu YJ, Liu YZ, Liang YJ, Feng GF, Zhang YP, et al. Effects of Chaihu-Shugan-San and Shen-Ling-Bai-Zhu-San on p38 MAPK pathway in Kupffer cells of nonalcoholic steatohepatitis. *Evid Based Complement Alternat Med* 2014;2014:671013.
- Shi XY, ed. *Experimental zoology of modern medicine*. Beijing: People's Military Medical Press;2000:334.
- Yang QH, Hu SP, Zhang YP, Ping HH, Yang HW, Chen TY, et al. Effects of different therapeutic methods and typical recipes of Chinese medicine on activation of c-Jun N-terminal kinase in Kupffer cells of rats with fatty liver disease. *Chin J Integr Med* 2012;18:769-774.
- Feng GF, Yang QH, Wang WJ, He XM, Zhang YP, Ji GY, et al. Simultaneously isolation and identification of hepatocytes and Kupffer cells from nonalcoholic steatohepatitis rat. *Guangdong Med J (Chin)* 2012;33:40-43.
- Cohen JC, Horton JD, Hobbs HH. Human fatty liver disease: old questions and new insights. *Science* 2011;332:1519-1523.
- Fuchs M. Non-alcoholic fatty liver disease: the bile acid-activated farnesoid x receptor as an emerging treatment target. *J Lipids* 2012;2012:934-396.
- Nseir W, Mahamid M. Statins in nonalcoholic fatty liver disease and steatohepatitis: updated review. *Curr Atheroscler Rep* 2013;15:1-6.
- Liaskou E, Wilson DV, Oo YH. Innate immune cells in liver inflammation. *Mediators Inflamm* 2012;2012:949157.
- Murray PJ, Wynn TA. Protective and pathogenic functions of macrophage subsets. *Nat Rev Immunol* 2011;11:723-737.
- Zimmermann HW, Trautwein C, Tacke F. Functional role of monocytes and macrophages for the inflammatory response in acute liver injury. *Front Physiol* 2012;19:3:56.
- Gao B. Cytokines, STATs and liver disease. *Cell Mol Immunol* 2005;2:92-100.
- Papackova Z, Palenickova E, Dankova H, Zdychova J, Skop V, Kazdova L, et al. Kupffer cells ameliorate hepatic insulin resistance induced by high-fat diet rich in monounsaturated fatty acids: the evidence for the involvement of alternatively activated macrophages. *Nutr Metab* 2012;9:22.
- Farrell GC, van Rooyen D, Gan L, Chitturi S. NASH is an inflammatory disorder: pathogenic, prognostic and therapeutic implications. *Gut Liver* 2012;6:149-171.
- Yang QH, Xu YJ, Feng GF, Hu CF, Zhang YP, Cheng

- SB, et al. p38 MAPK signal pathway involved in anti-inflammatory effect of Chaihu-shugan-san and Shen-ling-bai-zhu-san on hepatocyte in non-alcoholic steatohepatitis rats. *Afr J Tradit Complement Altern Med* 2014;11:213-221.
26. Fei ZW, Zhang XP, Zhang J, Huang XM, Wu DJ, Bi HH. Protective effects of *Radix Astragali* Injection on multiple organs of rats with obstructive jaundice. *Chin J Integr Med* 2016;22:674-684.
27. Takeda K, Akira S. TLR signaling pathways. *Semin Immunol* 2004;16:3-9.
28. Liu Y, Zhang Z, Wang L, Li J, Dong L, Yue W, et al. TLR4 monoclonal antibody blockade suppresses dextran-sulfate-sodium-induced colitis in mice. *J Gastroenterol Hepatol* 2010;25:209-214.
29. Alisi A, Panera N, Nobili V. Toll-like receptor 4: a starting point for proinflammatory signals in fatty liver disease. *Hepatology* 2010;51:714-715.
30. Luo JK, Zhou HJ, Wu J, Tang T, Liang QH. Electroacupuncture at Zusanli (ST 36) accelerates intracerebral hemorrhage-induced angiogenesis in rats. *Chin J Integr Med* 2013;19:367-373.
31. Qiao NL, Yang QH, Ji GY. A discussion on the view that Liver qi stagnation and Spleen deficiency is the basic pathogenesis of fatty liver. *Lishizhen Med Mater Med Res (Chin)* 2008;153:1238-1239.
32. Wei HF, JG, Xin LJ. Preliminary research on nonalcoholic fatty liver syndrome classification. *Liaoning J Tradit Chin Med (Chin)* 2002;29:655-656.
33. Zhang SS, Li QG, Li JX. Diagnosis and treatment of traditional Chinese medicine consensus on nonalcoholic fatty liver disease. *Beijing J Tradit Chin Med (Chin)* 2011;30:83-86.
34. Li L, Su DM, Han HX, Li JX. Traditional Chinese medicine for non-alcoholic steatohepatitis: a systematic review. *Chin J Evid Based Med (Chin)* 2011;11:195-203.
35. Ding T. Shenlingbaizhu Powder of ginseng saponin content determination. *Chin J Basic Med Tradit Chin Med (Chin)* 2012;10:1134-1135.
36. Wang CY, Zhang DS, Zhang WM, Guo CY, Xue GP. Determination of four effective components in Chaihu Shugan Powder by HPLC/DAD. *Chin Tradit Patent Med (Chin)* 2010;32:422-425.
37. Wang SL, Jia W, Gao XL. HPLC characteristics of aqueous extract of Chaihu Shugan Powder and determination of markers. *Chin Tradit Patent Med (Chin)* 2012;34:2384-2388.
38. Gong XW, Yang QH, Xu YJ. The effectiveness and safety of soothing Liver and activating Spleen method treating nonalcoholic fatty liver disease. *Chin J Gerontol (Chin)* 2014;14:3817-3820.
39. Gong XW, Yang QH, Xu YJ, Huang J. Medication rule for treating Liver depression and Spleen deficiency of fatty liver disease based on data mining. *Chin J Exp Tradit Med Formul (Chin)* 2013;19:344-348.
40. Li YQ, Yang QH, Xie WN, Ji GY. 35 patients with nonalcoholic fatty liver treatment of soothing Liver and invigorating Spleen method. *J Tradit Chin Med (Chin)* 2007;48:824-825.
41. Yang QH, Ou J, Sun SY, Qiao NL, Chen SB, Chen WQ, et al. Effects of soothing Liver and invigorating Spleen recipes on expression of PI3K p85 $\alpha$  protein in hepatocyte of rats with non-alcoholic fatty liver disease. *J Guangdong Pharmaceutical Coll (Chin)* 2009;25:62-67.
42. Gong XW, Han L, Yang QH, Yan HZ, Zhang YP, Li YY, et al. Effects of soothing Liver and invigorating Spleen recipe on lipid metabolism disorders in Kupffer cells of NAFLD rats by LXR $\alpha$ /SREBP-1c signal pathway. *Chin Herb Med* 2014;6:297-304.

(Accepted February 28, 2015; First Online January 9, 2018)

Edited by YU Ming-zhu